2023 IEEE/ASME International Conference on Advanced Intelligent Mechatronics (AIM)
June 28-30, 2023. Seattle, Washington, USA

Automated backlash determination on rack-and-pinion drives

Wiebke Zenn[1,*], Alexander Keck[2], Marcus Beck[3], Sven Herold[4] and Tobias Melz[4,5]

Abstract— **One characteristic of rack-and-pinion drives is that they are usually subject to backlash. In non-high precision applications, such as laser cutting, a certain amount of backlash is tolerated. However, changes in the amount of backlash are often related to a fault or damage in the machine. For this reason, it can be useful to monitor the size of the backlash. In this paper, a new method for the determination of backlash in rack-and-pinion drives is introduced and applied to single axes as well as to machines with gantry axes. Since in non-high precision applications there is generally no direct measuring system to detect the output-side position, an additional MEMS acceleration sensor is attached to the moving load. Its sensor signal is compared with the motor acceleration obtained from the differentiation of the measured motor speed during a positioning step. With these two acceleration signals, the beginning and the end of the change of the tooth flanks can be identified automatically considering the machine dynamics. From this, the size of the backlash can be determined. It is shown that an automated determination of the backlash is possible even for applications with highly complex machine dynamics.**

I. Introduction

The rack-and-pinion drive is one of the most common linear drives in the mechanical engineering industry. Due to its consistent stiffness, it is mainly used in large machines with long travel axes [1]. However, one main disadvantage of rack-and-pinion drives is the occurrence of backlash due to tolerances and manufacturing inaccuracies [2]. This results in a reduction of the positioning accuracy, which is why various techniques are used to reduce or compensate for this backlash in high-precision applications. In other areas, such as laser cutting machines, backlash within a certain tolerance is accepted, and in some cases even desired to avoid wear of all components. However, if the backlash value changes significantly, this usually indicates a fault or damage in the machine [3]. Therefore it can be useful to automatically monitor the size of the backlash.

Various methods for determining backlash were developed for gearboxes especially in the application of industrial robots. These methods differ in the required measurement signals and whether the evaluation is carried out in the time domain or in the frequency domain. In [4] and [5] methods in the frequency domain are shown, where changes of the frequency response functions due to backlash are evaluated, with and without the use of additional sensors. In the time domain, the methods can be further divided into direct and indirect methods. In the indirect methods, dynamic effects generated by the backlash are evaluated. In [6] and [7], for example, the influence of backlash on oscillations in the drive train is investigated. And [8] uses the relationship between the magnitude of backlash and the severity of tooth flank collision after a backlash pass.

In direct methods, the basic principle is to excite the system so that the pinion completely passes through the backlash gap, then to identify the beginning and end of this backlash pass, and to use this to determine the distance traveled in between. In [9] and [10] it is assumed that the backlash pass begins when the drive changes direction. For the identification of the re-engagement of the tooth flanks at the end of such a backlash pass, the measured motor current is evaluated. From the respective drive positions, the distance traveled in between is determined with the assumption that meanwhile the output is at rest. In [11] a similar method is shown, where the end of the backlash pass is identified by the motor speed and to determine the distance traveled, the output side is assumed to continue its movement with constant speed. Instead of making assumption for the output-side movement, [12] uses position measurement on the input and output sides as well as a gyroscope to detect tooth meshing, but such sensors are not available in every system. This problem is adressed in [3] where as a solution the use of a low-cost accelerometer is proposed, that can be placed at any location to detect the output-side motion. The determination of the beginning and the end of the backlash pass is done on the basis of the velocity curves. In all the procedures and methods mentioned, the backlash in gearboxes is investigated. In this work, however, the backlash of a rack-and-pinion drive is considered. For this purpose, a direct method in the time domain is developed. It is shown that the assumptions in [9] or [11] for the output-side motion and for the determination of the beginning of the backlash pass cannot be easily transferred to the system of a rack-and-pinion drive. Therefore, similar to [3], an additional output-side accelerometer is used to detect the output-side motion. In contrast to [3], the commutation times are evaluated directly using the acceleration signals. Since rack-and-pinion drives are often used in machine tools in conjunction with other axes, the method is extended not only for individual axes but also for so-called gantry drives. The developed algorithm is validated by simulations and experiments.

[1]W. Zenn is with TRUMPF Werkzeugmaschinen SE + Co. KG, Ditzingen, Germany, and is industrial doctoral student supervised by the Technical University of Darmstadt, Germany

[2]A. Keck is with TRUMPF TLSM GmbH, Ditzingen, Germany

[3]M. Beck is with WITTENSTEIN SE, Igersheim, Germany

[4]S. Herold and T. Melz are with the Fraunhofer Institute for Structural Durability and System Reliability LBF, Darmstadt, Germany

[5]T. Melz is with the Department for System Reliability Adaptive Structures and Machine Acoustics SAM, Technical University of Darmstadt, Germany

*Corresponding author wiebke.zenn@trumpf.com

978-1-6654-7633-1/23/$31.00 ©2023 IEEE

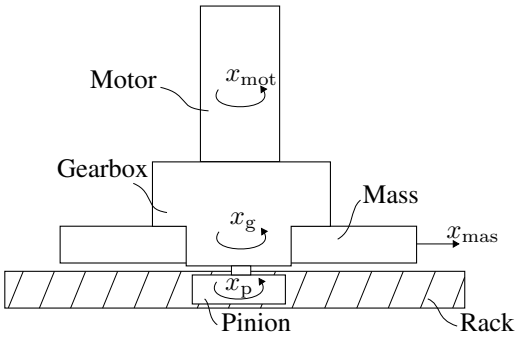

Fig. 1. Sketch of a rack and pinion drive

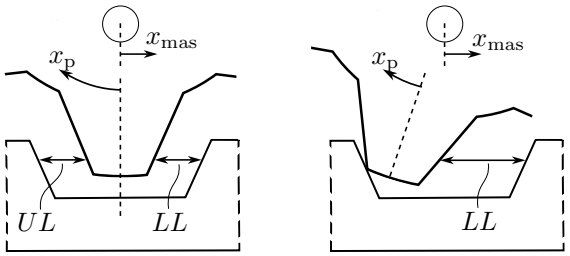

Fig. 2. Sketch of rack and pinion teeth with backlash of size b. Two exemplary initial positions: left with $|UL| = |LL| = \frac{1}{2}b$, right with $|UL| = 0$ and $|LL| = b$.

II. Dynamics of Backlash

The usual structure of a rack-and-pinion axis of a machine tool consists of a motor that drives a pinion via a gear. This pinion rolls on a fixed rack and thereby converts the rotation into a translational axis motion. A sketch of such a rack and pinion axis can be seen in Fig. 1.
For a single drive axis, this can be represented by the following equations of motion

$$\tau_{\mathrm{mot}} = J_{\mathrm{mot}}\ddot{x}_{\mathrm{mot}} + \tau_{\mathrm{mot,fric}} + \tau_{\mathrm{mot,compl}} \quad (1)$$

$$\tau_{\mathrm{mot,compl}} = J_{\mathrm{g}}\ddot{x}_{\mathrm{g}} + \tau_{\mathrm{g,fric}} + \frac{1}{i}\tau_{\mathrm{g,compl}} \quad (2)$$

$$\tau_{\mathrm{g,compl}} = J_{\mathrm{p}}\ddot{x}_{\mathrm{p}} + \tau_{\mathrm{p,fric}} + \frac{D_{\mathrm{p}}}{2}F_{\mathrm{p,compl}} \quad (3)$$

$$F_{\mathrm{p,compl}} = M\ddot{x}_{\mathrm{mas}} + F_{\mathrm{mas,fric}}. \quad (4)$$

Here τ_{mot} is the motor torque, J_{mot} the moment of inertia of the motor, $\ddot{x}_{\mathrm{mot}}$ the motor acceleration, $\tau_{\mathrm{mot,fric}}$ the friction torque in the motor and $\tau_{\mathrm{mot,compl}}$ the torque generated by the compliance of the connection between motor and gearbox. Similarly, the designations for the gearbox with index g, the pinion with index p and the translational moving mass with index mas apply. Translational forces are denoted by F. The translationally moved mass is modelles as mass point with weight M, i is the gear ratio and D_{p} is the pinion diameter.
The existence of backlash with size b between the pinion and the rack means that for some positions of the pinion relative to the rack, there is no power transmission to the load mass. This can be described by

$$F_{\mathrm{p,compl}} = k_{\mathrm{p}}\left(\Delta x^{\mathrm{b}}\right) + d_{\mathrm{p}}\left(\Delta \dot{x}^{\mathrm{b}}\right) \quad (5)$$

with k_{p} the pinion stiffness and d_{p} the pinion damping and

$$\Delta x^{\mathrm{b}} = \begin{cases} 0 & \text{if } \Delta x^{\mathrm{rp}} < UL \text{ and } \Delta x^{\mathrm{rp}} > LL \\ \Delta x^{\mathrm{rp}} - UL & \text{if } \Delta x^{\mathrm{rp}} > UL \\ \Delta x^{\mathrm{rp}} - LL & \text{if } \Delta x^{\mathrm{rp}} < LL, \end{cases} \quad (6)$$

and

$$\Delta \dot{x}^{\mathrm{b}} = \begin{cases} 0 & \text{if } \Delta x^{\mathrm{rp}} < UL \text{ and } \Delta x^{\mathrm{rp}} > LL \\ \Delta \dot{x}^{\mathrm{rp}} & \text{else.} \end{cases} \quad (7)$$

Here Δx^{b} describes the deadzone behaviour of systems with backlash. $\Delta x^{\mathrm{rp}} = \frac{D_{\mathrm{p}}}{2}x_{\mathrm{p}} - x_{\mathrm{mas}}$ is the translational difference between the pinion and the load mass. LL and UL are the distances from the pinion flanks to the respective rack tooth flanks at the initial position. For example, if the zero position is defined as the pinion tooth being exactly centered between two rack teeth, then $LL = -\frac{1}{2}b$ and $UL = \frac{1}{2}b$, as sketched in Fig. 2 left.

Neglecting the friction $\tau_{\mathrm{mas,fric}}$ in (4), it follows that for an acceleration of the load mass in positive direction of motion $F_{\mathrm{p,compl}} > 0$ must apply and consequently $\Delta x^{\mathrm{rp}} > UL$ according to (5) and (6). This means that the tooth flanks in the positive direction of motor rotation are in contact. For deceleration of the load mass it holds that $\tau_{\mathrm{p,compl}} < 0$ and therefore $\Delta x^{\mathrm{rp}} < LL$. This means that the tooth flanks are in contact in the negative direction of motor rotation.
During backlash, when the tooth flanks of the pinion and rack are not in contact at any point, the load mass and the drive train move separately. For a single drive axis, where the load can be modeled by a mass point, its dynamics is then purely dependent on the friction and the initial conditions at the time t_0 when the tooth flanks are loosened, such that

$$\begin{aligned} &M\ddot{x}_{\mathrm{mas}} = -F_{\mathrm{mas,fric}} \\ &\text{with } x_{\mathrm{mas}}(t_0) = x_{\mathrm{mas},0} \text{ and } \dot{x}_{\mathrm{mas}}(t_0) = v_{\mathrm{mas},0}. \end{aligned} \quad (8)$$

In machine tools, movements are often generated by an interaction of several drive axes whose dynamics influence each other. Also the moving axis can excite the machine body and other elastic elements. To investigate the influence of backlash on such machine drive axes, it is therefore generally not sufficient to approximate the load moved by the drive as a mass point. Rather, the influence of the entire chain of elastic mechanical elements on the translational motion of the pinion must be taken into account, whereby (4) extends to

$$F_{\mathrm{p,compl}} = m_{\mathrm{drive}}\ddot{x}_{\mathrm{mas}} + F_{\mathrm{mas,fric}} + f\left(\ddot{x}_{\mathrm{m1}}, \ddot{x}_{\mathrm{m2}}, ..., \ddot{x}_{\mathrm{mn}}\right) \quad (9)$$

where m_{drive} is then only the mass of the drive and $f\left(\ddot{x}_{\mathrm{m1}}, \ddot{x}_{\mathrm{m2}}, ..., \ddot{x}_{\mathrm{mn}}\right)$ describes the influence of n other moving components like the guide carriages, the machine body and other machine axes.

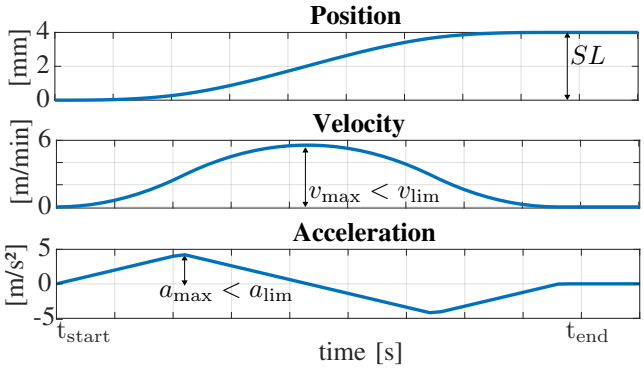

Fig. 3. Nominal Trajectory

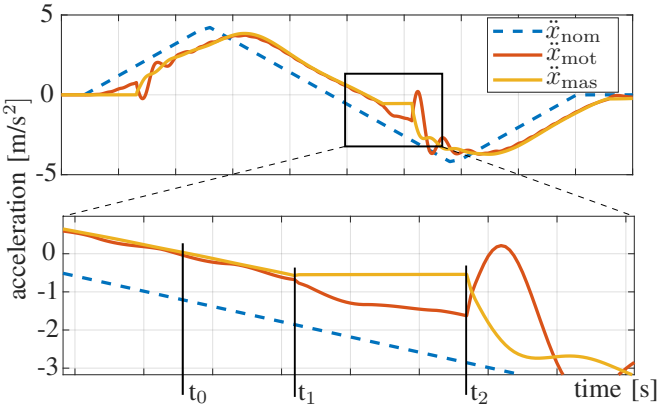

Fig. 4. Simulation results of a single rack and pinion drive with mass-point. Motor and mass acceleration during positioning step with backlash.

III. Backlash Determination

Based on the system dynamics described in Chapter II, a method for determining the size of the backlash b is shown in the following. First, a suitable excitation in the form of a nominal trajectory is selected. The requirements on the excitation trajectory are that the pinion runs through the backlash gap completely and that the start and end of this section are easily identifiable. In Section II it was described that the tooth flanks must be in contact in positive direction of motor rotation for acceleration of the load mass and in negative direction of motor rotation for braking. A tooth flank change therefore takes place during the transition from acceleration to braking, and the clearance is completely traversed. A trajectory often used on machine tools for diagnostic purposes, which contains this transition from acceleration to braking, is a jerk-limited positioning step. There the axis is translationally moved from standstill from a start position to a defined end position resulting in the steplength SL, while the jerk limit $j_{\lim}$, acceleration limit $a_{\lim}$ and the maximum permitted speed $v_{\lim}$ determine the course of the trajectory. All variables refer to the translational motion on the output side. Such a movement also occurs frequently during normal operation of a machine tool. Fig. 3 shows such an trajectory. For this nominal trajectory it should hold that $v_{\max} < v_{\lim}$ such that between the acceleration and braking phases there is no section of zero acceleration but there is one clear point of time when the acceleration changes the sign. Also the detection of the beginning and the end of the backlash pass can be improved when $j_{\lim}$ is large but it may only be selected so large that the time for passing through the backlash gap is much greater that the sampling time of the measurement signals.

To determine the backlash, such a nominal trajectory is applied as reference trajectory to the controlled axis. The controller has a, for machine tool axes usual, PPI cascade structure with the input variables of motor position, the motor speed and the motor current. Fig. 4 shows the resulting acceleration curves of the motor and the moving load mass. As described in [3], there are two sections in which the backlash becomes visible. One at the beginning of the motion, when the motor is moving but the load mass remains stationary until the backlash gap has been passed and the pinion meshes with the rack. The second backlash-dependent section occurs when the motor movement changes from acceleration to braking. Here, as previously described, a tooth flank change takes place and the backlash gap is completely traversed. During this section, there is no power transfer from the drive to the load mass, so the motion of the load mass diverge from that of the motor (8) until the tooth flanks collide again. As described in [3], the first section can be used to determine the backlash if the initial position of the pinion relative to the rack is known, and in the best case is such that the entire backlash must be traversed at the beginning of the motion. Since this is not generally the case on machine tool axes, only the second section is used here to determine the backlash.

In order to determine the size of the backlash from this section, the starting time t_1 and finishing t_2 of the pinion being in no contact with the rack must be identified. The distance covered in between can be referred to the size of the backlash $b = \bar{x}_{\text{mot}}(t_2) - x_{\text{mas}}(t_2) - (\bar{x}_{\text{mot}}(t_1) - x_{\text{mas}}(t_1))$ with $\bar{x}_{\text{mot}} = \frac{D}{2i} x_{\text{mot}}$ being the to the output-side converted motor position. The motor position is generally given via a motor encoder. However, the load mass position is unknown in many machine tools that are not used for high-precision manufacturing. [11] estimates the load mass position by assuming that its velocity is the same as the motorspeed when the tooth flanks are loosened, and that it then remains constant during backlash. As [3] describes, this assumption leads to errors for machines whose axes are subject to friction and are affected by other axes and vibrations in the machine. A convenient way to get this missing information about the movement of the load mass is by using an accelerometer. It must be attached to the moving load, preferably close to the pinion, and measure the acceleration in the direction of motion of the load mass $\ddot{x}_{\text{mas}}$. The size of the backlash can then be calculated using

$$b = \bar{x}_{\text{mot}}(t_2) - \bar{x}_{\text{mot}}(t_1) - \iint_{t_1}^{t_2} \ddot{x}_{\text{mas}} \, \mathrm{d}t^2. \qquad (10)$$

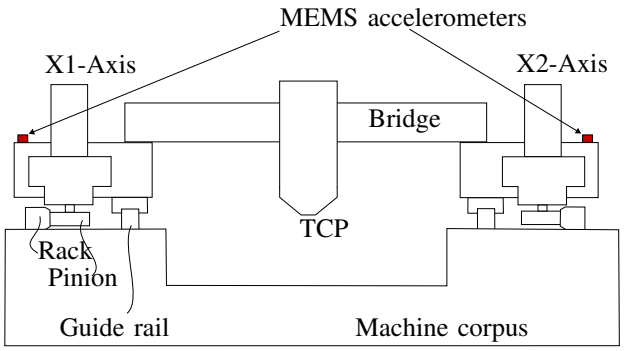

Fig. 5. Sketch of machine tool with gantry axis

Since a drift generally falsifies the results when integrating sensor data, suitable filtering methods must be used here depending on the acceleration sensor.

For utilization of (10) the commutation times t_1 and t_2 must first be identified. Therefore the motor acceleration is calculated from the motor sensor data by differentiation and is directly compared with the mass acceleration as shown in Fig. 4. From the comparison of these two acceleration curves, the time points t_1 and t_2 can be determined. The time t_1 is when $\frac{D_\mathrm{p}}{2} x_\mathrm{p}(t) - x_\mathrm{mas}(t)$ is first greater than or equal to LL. For applications as in [11] and [3] this moment occurs at the same time when the motor starts the braking process at t_0. However, in the case of the rack-and-pinion axis investigated here, it was found that this point in time t_1 is not equal to time of the sign change in the motor acceleration t_0 due to compliance of all components and friction in the guide. For a single axis the time period between t_0 and t_1 can be assumed to be almost constant, provided that the stiffnesses, dampings and frictions are not subject to significant variations. Therefore, the time t_1 for such a system can be determined either from the system's equations of motion if the parameters are known or by experiments. If the friction is very low, it may also be possible to assume that $t_0 = t_1$.

Considering an entire machine instead of a single axis, the influence of other axes on the pinion dynamics must be taken into account. Fig. 5 shows a sketch of a laser cutting machine in which the axes X1 and X2 form a so-called gantry unit. This consists of two parallel running axes, each with its own drive, that move the bridge in between. The drives are identical rack-and-pinion drives each with its own controller. Here, the two parallel drives influence each other. For example the backlash may be different on both sides or the initial positions of the pinions with respect to the racks are not the same, as seen in Fig 6. Despite the same target trajectory this can result in different translational axis positions. In this case, one axis acts on the other as a tractive force in or against the direction of travel. This can increase or decrease the time when the tooth flanks disengage. Therefore the time period between t_0 and t_1 cannot be assumed as constant and cannot be determined in general terms by experiments or via the transfer functions.

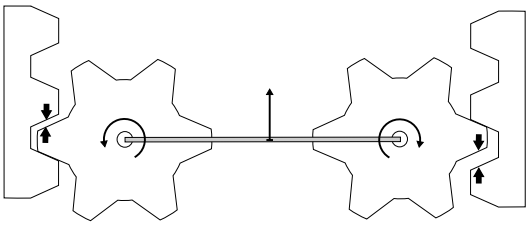

Fig. 6. Sketch of a rack-and-pinion gantry axis with different backlash sizes and zero positions of the pinions w.r.t. the racks

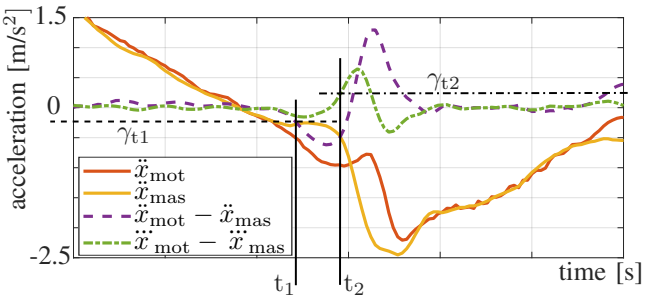

Fig. 7. Measured acceleration curves on machine with gantry rack and pinion drive during positioning step and auxiliary curves for the identification of commutation times.

However, it is still the case that from the time when the tooth flanks separate from each other, the motor acceleration and the mass acceleration diverge. The resulting difference between motor acceleration and mass acceleration can be used as an approximate indicator for the start of the backlash

$$\ddot{x}_\mathrm{mot}(t) - \ddot{x}_\mathrm{mas}(t) < \gamma_{t1} \quad \forall\, t > t_1 \tag{11}$$

with γ_{t1} being a threshold indicating the beginning of the backlash section. The threshold must be chosen manually for a robust identification. It mainly depends on the jerk limit of the nominal trajectory and is independent from the application and the backlash size.

After traversing the backlash gap, the tooth flanks of the pinion and the rack meet again. Since at this point the translational speed differ from the rotational speed of the pinion, the load mass is abruptly decelerated, the pinion and thus also the motor are accelerated in the direction of rotation. This sudden change in the acceleration curves can be used as an indicator for the end of the backlash gap.

$$\dddot{x}_\mathrm{mot}(t) - \dddot{x}_\mathrm{mas}(t) > \gamma_{t2} \quad \forall\, t > t_2. \tag{12}$$

Since this change in the acceleration curves depends on the velocity difference of the rack and the moved mass at the commutation time, it can be more robust to use the maximum of the acceleration change instead of one fixed value, e.g. the threshold $\gamma_{t2} = 0.5 \max(\dddot{x}_\mathrm{mot} - \dddot{x}_\mathrm{mas})$.

Fig. 7 shows the acceleration curves of one axis of a machine with gantry unit, and the indicator curves with the thresholds for determining the beginning and end of the backlash section.

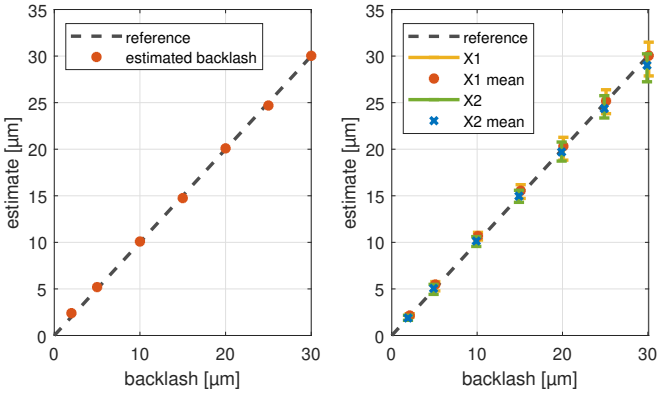

Fig. 8. Estimated backlash for drive train simulation model (left) and for full machine simulation model with different backlash sizes and zero positions on both axes (right).

IV. Simulation Model and Results

The previously explained method for determining rack-and-pinion backlash is implemented, tested and evaluated using a simulation model.

First, a model of a single rack-and-pinion axis was created in MATLAB/SIMULINK. The model consists of a controller, which is a PPI cascade controller analogous to standard machine controllers. The controlled system is a rigid-body model with elastic joints consisting of a motor model, gearbox and pinion. Via the pinion, the rotation is converted to a translatory motion. In addition to compliance and friction, the backlash is also modeled here as in (5) to (7). The translational moving load mass is approximated by a simple frictional mass point. The dynamics of the system plant is equivalent (1) to (4). The axis is only controlled by the motor measurement system. For backlash determination, however, the acceleration of the mass point is available in addition to motor current and motor speed. The target trajectory was chosen as derived in Chapter III as a positioning step with a step size of $SL = 4$ mm and a jerk limit of $j_{\mathrm{lim}} = 200\ \mathrm{m/s^4}$.

For this nominal trajectory, the motor acceleration and load mass acceleration at different sizes of backlash were simulated. Example acceleration curves are shown in Fig. 4. From these acceleration curves, as described in Chapter III, the start time of the backlash pass t_1 according to (11) and the end time of the backlash run t_2 according to (12) is identified. From this times and the acceleration signals the size of the covered distance and thus of the backlash can now be determined according to (10). For such numeric calculated noiseless signals filtering is not necessary. Fig. 8 left shows the calculated backlash values compared with the actual values. It becomes clear that for a single axis this algorithm allows the a very precise determination of the backlash.

As described before the behavior becomes much more complicated as soon as not only a single axis but a whole machine is considered. For simulative testing of backlash determination for such a machine, a simulation model in MATLAB/SIMULINK is used of an entire machine as sketched in Fig. 5. It consists of a gantry unit as explained in Chapter III being two parallel axes with identical drives, each modelled the same as in the simulation model of the single axis. The motion is controlled on the basis of the respective motor encoders. The flexible components, as the carriage guides, the bridge and the machine corpus are derived from finite-element-models. Various scenarios can now occur: There may be different amounts of backlash on the two axes, the initial position between pinion and rack can vary on both axes and there can be differences in the friction of both axes. Therefore for each X-axis, the friction curve, the size of backlash and the zero position between pinion and rack can be specified. The motor speeds are again available as system outputs and a point on each carriage guide is selected for the output-side accelerations. Positioning steps are simulated according to the same nominal trajectory as for the single axis and the algorithm for backlash determination is applied as before. Fig. 8 right shows the comparison between the determined and the actual backlash for different backlash sizes and zero positions between rack and pinion teeth.

Due to the presence of different amounts of backlash and different initial positions, the backlash on both sides is not passed through simultaneously. However, since the two axes are connected by mechanical components, their movements influence each other. This results in overlaps that make it much more difficult to identify the beginning and end of the backlash gap. Therefore this algorithm can only achieve an accuracy of ± 1 % of the backlash size.

V. Experimental Set-up and Results

A laser cutting machine from TRUMPF Machine Tools was used for the experimental validation. The experiment is set up as shown in Fig. 5 and has a gantry-axis with rack-and-pinion drives in the X direction. The drives each consist of a Siemens motor and a Wittenstein gear unit with an add-on pinion. They are controlled via the Siemens SL840d control system. In addition to the motor encoder, a MEMS acceleration sensor from Kistler is attached to the carriage on each X-axis for acceleration measurement on the output side as also sketched in Fig. 5.

For different backlash sizes and zero positions of the two axes, positioning steps are again performed which fulfill the conditions from Chapter III and the backlash is determined using the measured motor speed and the output acceleration measured with the additional accelerometers. To minimize measurement inaccuracies one experiment consists of ten steps which results are averaged. For the identification of the start and end of the backlash interval the motorspeed is differentiated and smoothed with a sawitzky-golay-filter. For the ingetration the motorencoder signals and the accelerometer signals are both lowpass filtered with a 10th order butterworth filter. To determine the quality of the backlash determination, the actual backlash value is required. For this purpose, a direct displacement measuring system, for example a measuring probe, is mounted on the output

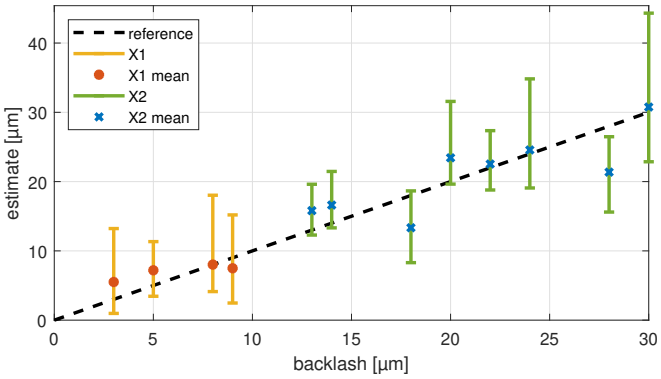

Fig. 9. Estimated backlash for experiments on cutting laser machine. Different backlash sizes and zero positions on both axes.

side and the backlash measured via the displacement during manual force application. Due to measurement inaccuracies the reference backlash values have already an uncertainty of approximately $\pm 2\ \mu\mathrm{m}$.

Fig. 9 shows the backlash values determined from the acceleration data over the manually measured reference backlash values. The figure shows that, for the measurement the variation of the determined backlash vary much more than in the simulation. However for one measuring position the mean of all determined backlash values is close to the manually measured reference value. Also the uncertainty of the reference value may influence the results. In this experiment the backlash determination algorithm achieved an accuracy of approximately $\pm 20\ \%$ of the backlash size.

VI. Discussion

In this work, a new method was derived to automatically determine the backlash on rack-and-pinion drives. Special attention was paid to machine tool applications with multiple axes. In addition to the selection of a suitable trajectory, the innovation of this method is the identification of the beginning and the end of the backlash section on the basis of acceleration signals of the motor and the translational moving mass. For the measurement of this output side acceleration, an accelerometer is attached to the moving mass. Here, for example, inexpensive MEMS sensors can be additionally attached. A particularly convenient solution is also the use of sensors already built into components as there is a gearbox manufacturer that offer an acceleration sensor built into the gearbox housing.

For a single rack-and-pinion axis the algorithm allows a precise determination of the backlash size. When transferring the backlash determination algorithms to an entire machine, in particular to a gantry axis unit, the influence of the axes on each other must be taken into account. The accuracy of the estimated backlash size decreases significantly. Deviations in the estimation arise primarily from the fact that the start and end times of the backlash section can only be identified inaccurately in some cases due to the superposition of the two axis motions. In particular, the choice of one fixed threshold to determine these times for all scenarios of backlash sizes and zero positions is difficult here. One possibility to become more precise here is the use of machine-learning methods to determine these points in time. Further inaccuracies arise from the drift in the integration of sensor signals, which has a particular impact on small backlash sizes. Here, extended filtering methods could increase the quality of the backlash estimation. For the use in automatic monitoring of the backlash on a laser cutting machine, the accuracy achieved is sufficient to diagnose strong changes in the backlash that indicate an undesirable condition of the machine and, if necessary, to assist a service technician by providing location information of critical areas. Only when higher accuracy can be achieved such an algorithm could completely replace manual measurement in the future.

Acknowledgment

This project (ProKInect N° 02P20A090) is funded by the German Federal Ministry of Education and Research (BMBF) within the "The Future of Value Creation – Research on Production, Services and Work" program and managed by the Project Management Agency Karlsruhe (PTKA). The support is greatly acknowledged. The authors are responsible for the content of this publication.

References

[1] C. Ehrmann, P. Isabey, and J. Fleischer, "Condition monitoring of rack and pinion drive systems: Necessity and challenges in production environments," in *13th Global Conference on Sustainable Manufacturing*, vol. 40, 2016, pp. 197–201.

[2] A. Engelberth, S. Apprich, J. Friedrich, *et al.*, "Properties of electrically preloaded rack-and-pinion drives," *Production Engineering*, vol. 9, p. 269–276, 2015.

[3] M. Tantau, L. Perner, M. Wielithka, and T. Ortmaier, "Backlash identification in industrial positioning systems aided by a mobile accelerometer board with wi-fi," in *Proceedings of the 17th International Conference on Informatics in Control, Automation and Robotics (ICINCO 2020)*, Prague, 2020, pp. 576–584.

[4] N. G. Dagalakis and D. R. Myers, "Adjustment of robot joint gear backlash using the robot joint test excitation technique," *The International Journal of Robotics Research*, vol. 4, no. 2, pp. 65–79, 1985.

[5] E. Popp, M. Tantau, M. Wielitzka, *et al.*, "Frequency domain identification and identifiability analysis of a nonlinear vehicle drivetrain model," in *18th European Control Conference (ECC)*, 2019, pp. 237–242.

[6] N. Sarkar, R. E. Ellis, and T. N. Moore, "Backlash detection in geared mechanisms: Modeling, simulation, and experimentation," in *Mechanical Systems and Signal Processing*, vol. 11, no. 3, 1997, pp. 391–408.

[7] E. Giovannitti *et al.*, "A virtual sensor for backlash in robotic manipulators," *Journal of Intelligent Manufacturing*, vol. 33, p. 1921–1937, 2022.

[8] J. L. Stein and C. Wang, "Estimation of gear backlash: Theory and simulation," *Journal of Dynamic Systems, Measurement and Control*, vol. 120, pp. 74–82, 1998.

[9] D. Gebler and J. Holtz, "Identification and compensation of gear backlash without output position sensor in high-precision servo systems," in *Proc. IEEE Annu. Conf. Ind. Electron. Soc. (IECON)*, 1998, pp. 662–666.

[10] L. Marton and B. Lantos, "Friction and backlash measurement and identification method for robotic arms," in *2009 International Conference on Advanced Robotics*, 2009.

[11] S. Villwock and M. Pacas, "Deterministic method for the identification of backlash in the time domain," in *Proc. IEEE ISIE Conf.*, 2006, pp. 3056–3061.

[12] M. Li, R. Liang, Y. Zhang, C. Peng, D. Mu, and Z. Wan, "Online measurement method of transmission backlash based on angular velocity and double-end angular position information," *Measurement and Control*, vol. 54, pp. 65–72, 2021.